within the proximal promoter of PXR. Drug Metab Dispos 2006;34:138-144.

30. Enjoji M, Yada R, Fujino T, Yoshimoto T, Yada M, Harada N, Higuchi N, et al. The state of cholesterol metabolism in the liver of patients with primary biliary cirrhosis: the role of MDR3 expression. Hepatol Int 2009.

31. Nakamuta M, Fujino T, Yada R, Yasutake K, Yoshimoto T, Harada N, Yada M, et al. Therapeutic effect of bezafibrate against biliary damage: a study of phospholipid secretion via the PPARα-MDR3 pathway. Int J Clin Pharmacol Ther 2010;48:22-28.

32. Marrapodi M, Chiang JY. Peroxisome proliferator-activated receptor a (PPARα) and agonist inhibit cholesterol 7α-hydroxylase gene (CYP7A1) transcription. J Lipid Res 2000;41:514-520.

33. Post SM, Duez H, Gervois PP, Staels B, Kuipers F, Princen HM. Fibrates suppress bile acid synthesis via peroxisome proliferator-activated receptor-alpha-mediated downregulation of cholesterol 7α-hydroxylase and sterol 27-hydroxylase expression. Arterioscler Thromb Vasc Biol 2001;21:1840-1845.

34. Stedman C, Liddle C, Coulter S, Sonoda J, Alvarez JG, Evans RM, Downes M. Benefit of farnesoid X receptor inhibition in obstructive cholestasis. Proc Natl Acad Sci USA 2006;103:11323-11328.

35. Assem M, Schuetz EG, Leggas M, Sun D, Yasuda K, Reid G, Zelcer N, et al. Interactions between hepatic Mrp4 and Sult2a as revealed by the constitutive androstane receptor and Mrp4 knockout mice. J Biol Chem 2004;279:22250-22257.

36. Renga B, Migliorati M, Mencarelli A, Cipriani S, D'Amore C, Distrutti E, Fiorucci S. Farnesoid X receptor suppresses constitutive androstane receptor activity at the multidrug resistance protein-4 promoter. Biochim Biophys Acta 2011;1809:157-165.

37. Diczfalusy U, Nylen H, Elander P, Bertilsson L. 4β-hydroxycholesterol, an endogenous marker of CYP3A4/5 activity in humans. Br J Clin Pharmacol 2011;71:183-189.

38. Kajosaari LI, Backman JT, Neuvonen M, Laitila J, Neuvonen PJ. Lack of effect of bezafibrate and fenofibrate on the pharmacokinetics and pharmacodynamics of repaglinide. Br J Clin Pharmacol 2004;58:390-396.

39. Faucette SR, Sueyoshi T, Smith CM, Negishi M, Lecluyse EL, Wang H. Differential regulation of hepatic CYP2B6 and CYP3A4 genes by constitutive androstane receptor but not pregnane X receptor. J Pharmacol Exp Ther 2006;317:1200-1209.

40. Staudinger JL, Goodwin B, Jones SA, Hawkins-Brown D, Mackenzie KI, LaTour A, Liu Y, et al. The nuclear receptor PXR is a lithocholic acid sensor that protects against liver toxicity. Proc. Natl. Acad. Sci. USA 2001;98:3369-3374.

41. Xie W, Radominska-Pandya A, Shi Y, Simon CM, Nelson MC, Ong ES, Waxman DJ, et al. An essential role for nuclear receptors SXR/PXR in detoxification of cholestatic bile acids. Proc. Natl. Acad. Sci. USA 2001;98:3375-3380.

42. Synold TW, Dussault I, Forman BM. The orphan nuclear receptor SXR coordinately regulates drug metabolism and efflux. Nat Med 2001;7:584-590.

43. Kast HR, Goodwin B, Tarr PT, Jones SA, Anisfeld AM, Stoltz CM, Tontonoz P, et al. Regulation of multidrug resistance-associated protein 2 (ABCC2) by the nuclear receptors pregnane X receptor, farnesoid X-activated receptor, and constitutive androstane receptor. J Biol Chem 2002;277:2908-2915.

44. Li T, Chiang JYL. Mechanism of rifampicin and pregnane X receptor (PXR) inhibition of human cholesterol 7α-hydroxylase gene (CYP7A1) transcription. Am J Physiol 2005;288:G74-G84.

45. De Fabiani E, Mitro N, Gilardi F, Caruso D, Galli G, Crestani M. Coordinated control of cholesterol catabolism to bile acids and of gluconeogenesis via a novel mechanism of transcription regulation linked to the fasted-to-fed cycle. J Biol Chem 2003;278:39124-39132.

46. Bachs L, Pares A, Elena M, Piera C, Rodes J. Effects of long-term rifampicin administration in primary biliary cirrhosis. Gastroenterology 1992;102:2077-2080.

47. Prince MI, Burt AD, Jones DE. Hepatitis and liver dysfunction with rifampicin therapy for pruritus in primary biliary cirrhosis. Gut 2002;50:436-439.

48. Zimmermann C, van Waterschoot RA, Harmsen S, Maier A, Gutmann H, Schinkel AH. PXR-mediated induction of human CYP3A4 and mouse Cyp3a11 by the glucocorticoid

budesonide. Eur J Pharm Sci 2009;36:565-571.

49. Sorokin A, Brown JL, Thompson PD. Primary biliary cirrhosis, hyperlipidemia, and atherosclerotic risk: a systematic review. Atherosclerosis 2007;194:293-299.
50. Stahlberg D, Reihner E, Rudling M, Berglund L, Einarsson K, Angelin B. Influence of bezafibrate on hepatic cholesterol metabolism in gallstone patients: reduced activity of cholesterol 7α-hydroxylase. Hepatology 1995;21:1025-1030.
51. Roglans N, Vazquez-Carrera M, Alegret M, Novell F, Zambon D, Ros E, Laguna JC, et al. Fibrates modify the expression of key factors involved in bile-acid synthesis and biliary-lipid secretion in gallstone patients. Eur J Clin Pharmacol 2004;59:855-861.
52. Raedsch R, Plachky J, Wolf N, Simonis G. Biliary lipids, lithogenic index and biliary drug concentrations during etofibrate and bezafibrate treatment. Eur J Drug Metab Pharmacokinet 1995;20:113-118.
53. Caroli-Bosc FX, Le Gall P, Pugliese P, Delabre B, Caroli-Bosc C, Demarquay JF, Delmont JP, et al. Role of fibrates and HMG-CoA reductase inhibitors in gallstone formation: epidemiological study in an unselected population. Dig Dis Sci 2001;46:540-544.
54. Wallace K, Cowie DE, Konstantinou DK, Hill SJ, Tjelle TE, Axon A, Koruth M, et al. The PXR is a drug target for chronic inflammatory liver disease. J Steroid Biochem Mol Biol 2010;120:137-148.
55. Li MD, Yang X. A Retrospective on Nuclear Receptor Regulation of Inflammation: Lessons from GR and PPARs. PPAR Res 2011;2011:742785.

## Figure legends

**Fig. 1.** Effects of UDCA and additional bezafibrate treatment on serum liver enzymes (a) and lipids (b). B, before treatment; A, after treatment; BF, bezafibrate; T-CHOL, total cholesterol; LDL, LDL cholesterol; HDL, HDL cholesterol; TG, triglyceride. The mean concentrations before treatment were set to 1.0, and the absolute concentrations before treatment are shown in Table 1. Data are expressed as the mean±SEM.

**Fig. 2.** Effects of UDCA and additional bezafibrate treatment on bile acid metabolism. (a) C4, 7α-hydroxy-4-cholesten-3-one; FGF19, fibroblast growth factor 19; B, before treatment; A, after treatment; BF, bezafibrate. Mean concentrations before treatment (ng/mg cholesterol for C4 and pg/ml for FGF19) were set to 1.0, and the absolute concentrations before treatment are shown in Table 2. Data are expressed as the mean±SEM. (b) Serum concentrations of bile acids in UDCA treated patients before and after addition of bezafibrate (n=17). (c) Serum proportions of UDCA in UDCA treated patients before and after addition of bezafibrate (n=17). The mean value for each group is indicated by the columns. Free BA, unconjugated bile acids; Glyco-BA, glycine-conjugated bile acids; Tauro-BA, taurine-conjugated bile acids.

**Fig. 3.** Effect of UDCA and additional bezafibrate treatment on cholesterol (a) and oxysterol (b) metabolism. B, before treatment; A, after treatment; BF, bezafibrate; 4β-HC, 4β-hydroxycholesterol; 24S-HC, 24S-hydroxycholesterol; 27-HC, 27-hydroxycholesterol. Mean concentrations before treatment (μg/mg cholesterol or ng/mg cholesterol) were set to 1.0, and the absolute concentrations before treatment are shown in Table 2. Data are expressed as the mean±SEM.

**Fig. 4.** Effects of bezafibrate, rifampicin, carbamazepine and GW4064 on the activation of CYP3A4 and human PXR. (a) HepaRG cells were treated with each compound for 48 hrs in triplicate. mRNA expression levels were standardized to those of β-actin. The mean expression and activity levels in control cells were set to 1.0. Data are expressed as the mean±SD. Effects of bezafibrate are shown as the solid bars. *, †, ‡ $P<0.05$, 0.005, 0.001, respectively, indicate significant difference from controls. (b) DPX2 cells were treated with each compound for 24 hrs in triplicate. Activation of human PXR was determined by a cell-based luciferase reporter gene assay. The average relative luminescent units (RLU) obtained with the DMSO solvent control was set to 1.0.

**Fig. 5.** Effects of bezafibrate, rifampicin, carbamazepine and GW4064 on mRNA expression levels of nuclear receptors and a related coactivator (a), transporters (b) and enzymes and LDL receptor (c) in HepaRG cells. The cells were treated with each compound for 48 hrs, in triplicate. mRNA expression levels were standardized to those of β-actin. The mean expression and activity levels in control cells were set to 1.0. Data are expressed as the mean±SD. The effects of bezafibrate are shown as the solid bars. C, control; 10, bezafibrate 10 μM; 50, bezafibrate 50 μM; 100, bezafibrate 100 μM; 200, bezafibrate 200 μM; R, rifampicin 10 μM; M, carbamazepine 50 μM; G, GW4064 3 μM. PPARα, peroxisome proliferator-activated receptor α; PXR, pregnane X receptor; FXR, farnesoid X receptor; SHP, small heterodimer partner; FTF, α-fetoprotein transcription factor; HNF4α, hepatocyte nuclear factor 4α; PGC1α, peroxisome proliferator-activated receptor γ coactivator 1α; LXRα, liver X receptor α; MDR, multidrug resistance protein; MRP, multidrug resistance-associated protein; ABC, ATP-binding cassette transporter; NTCP, $Na^+$/taurocholate-cotransporting polypeptide; CYP7A1, cholesterol

7α-hydroxylase; CYP7B1, oxysterol 7α-hydroxylase; CYP8B1, 7α-hydroxy-4-cholesten-3-one 12α-hydroxylase; CYP27A1, sterol 27-hydroxylase; HMGCR, HMG-CoA reductase; LDLR, LDL receptor; ACC1, acetyl-CoA carboxylase 1; FAS, fatty acid synthase. *, †, ‡ $P<0.05$, 0.005, 0.001, respectively, indicate significant difference from control.

**Fig. 6.** Regulation of hepatic transporter activities and bile acid metabolism by PPARs, PXR and UDCA. Bezafibrate is a dual agonist of both PPARs and PXR. The activation of PPARs inhibits CYP7A1, CYP27A1 and NTCP, and upregulates MDR3 and presumably ABCG5/G8. The activation of PXR inhibits CYP7A1 and stimulates CYP3A4, MDR1 and MRP2. Genes that are downregulated by PPARs or PXR are indicated by the red lines, while those that are upregulated by PPARs, PXR or UDCA are indicated by the green arrows.

**Table 1. Characteristics of Patients with PBC Enrolled in the Present Study**

| Laboratory data | Control (n=49) | Before UDCA treatment (n=31) | Before BF treatment (n=19) |
|---|---|---|---|
| Age (yrs) | 57.8±1.6 [22-79] | 60.3±1.8 [37-81] | 58.8±1.6 [45-73] |
| Gender (Male/Female) | 11/38 | 4/27 | 1/18 |
| AST (IU/L) | 21±1 [11-34] | 64±18‡ [19-120] | 45±5‡ [20-101] |
| ALT (IU/L) | 17±1 [7-30] | 82±34‡ [12-138] | 51±9‡ [18-152] |
| GGT (IU/L) | 25±2 [7-58] | 196±27‡ [30-757] | 178±59‡ [47-445] |
| ALP (IU/L) | 230±9 [126-336] | 517±43‡ [229-1163] | 597±51‡ [266-952] |
| Total bilirubin (mg/dL) | 0.7±0.1 [0.3-1.2] | 0.7±0.2 [0.3-1.3] | 0.6±0.1 [0.3-1.1] |
| IgM (mg/dL) | 97±12 [56-161] | 288±27‡ [90-637] | 306±60† [130-466] |
| Total cholesterol (mg/dL) | 199±4 [130-257] | 213±9 [120-356] | 228±18 [118-343] |
| LDL cholesterol (mg/dL) | 115±4 [46-194] | 138±7* [91-254] | 149±18 [54-228] |
| HDL cholesterol (mg/dL) | 65±2 [33-111] | 53±4* [13-95] | 55±5 [13-89] |
| Triglycerides (mg/dL) | 91±6 [33-214] | 107±7* [47-199] | 113±11 [40-243] |

Data are expressed as mean±SEM [range].

Before UDCA treatment, all PBC patients before treatment with UDCA; Before BF treatment, PBC patients who exhibited an incomplete biochemical response to the UDCA monotherapy (600 mg/day) and before additional treatment with bezafibrate.

*P<0.05, significantly different from control.

†P<0.005, significantly different from control.

‡P<0.0001, significantly different from control.

**Table 2. Baseline Biomarker Levels for Cholesterol Metabolism in Enrolled Patients with PBC**

| Serum biomarkers | Control (n=49) | Before UDCA treatment (n=31) | Before BF treatment (n=19) |
|---|---|---|---|
| Bile acid metabolism | | | |
| C4 (ng/mg CHOL) | 15.7±2.9 [2.3-118] | 12.1±1.8 [0.8-49] | 11.8±2.1 [1.5-38] |
| FGF19 (pg/ml) | 336±51 [50-1662] | 309±49 [74-1543] | 353±57 [114-930] |
| Cholesterol metabolism | | | |
| Lathosterol (μg/mg CHOL) | 2.8±0.3 [0.9-11.7] | 2.2±0.2 [0.7-5.8] | 2.2±0.3 [0.8-6.1] |
| Sitosterol (μg/mg CHOL) | 1.6±0.1 [0.4-3.8] | 2.0±0.2* [0.8-3.9] | 2.4±0.2† [1.1-4.3] |
| Campesterol (μg/mg CHOL) | 1.8±0.1 [0.4-5.1] | 2.0±0.1 [0.7-3.7] | 1.9±0.2 [0.7-3.3] |
| Oxysterol metabolism | | | |
| 4β-HC (ng/mg CHOL) | 29±3 [11-135] | 44±4‡ [24-140] | 51±5‡ [20-92] |
| 24S-HC (ng/mg CHOL) | 31±2 [17-74] | 34±2 [22-69] | 41±2†[20-64] |
| 27-HC (ng/mg CHOL) | 77±3 [35-140] | 75±4 [48-124] | 75±4 [39-102] |

Data are expressed as mean±SEM [range].

Before UDCA treatment, all PBC patients before treatment with UDCA; Before BF treatment, PBC patients who exhibited an incomplete biochemical response to the UDCA monotherapy (600 mg/day) and before additional treatment with bezafibrate; C4, 7α-hydroxy-4-cholesten-3-one; CHOL, cholesterol; FGF19, fibroblast growth factor 19; 4β-HC, 4β-hydroxycholesterol; 24S-HC, 24S-hydroxycholesterol; 27-HC, 27-hydroxycholesterol.

*P<0.05, significantly different from control.

†P<0.005, significantly different from control.

‡P<0.0001, significantly different from control.

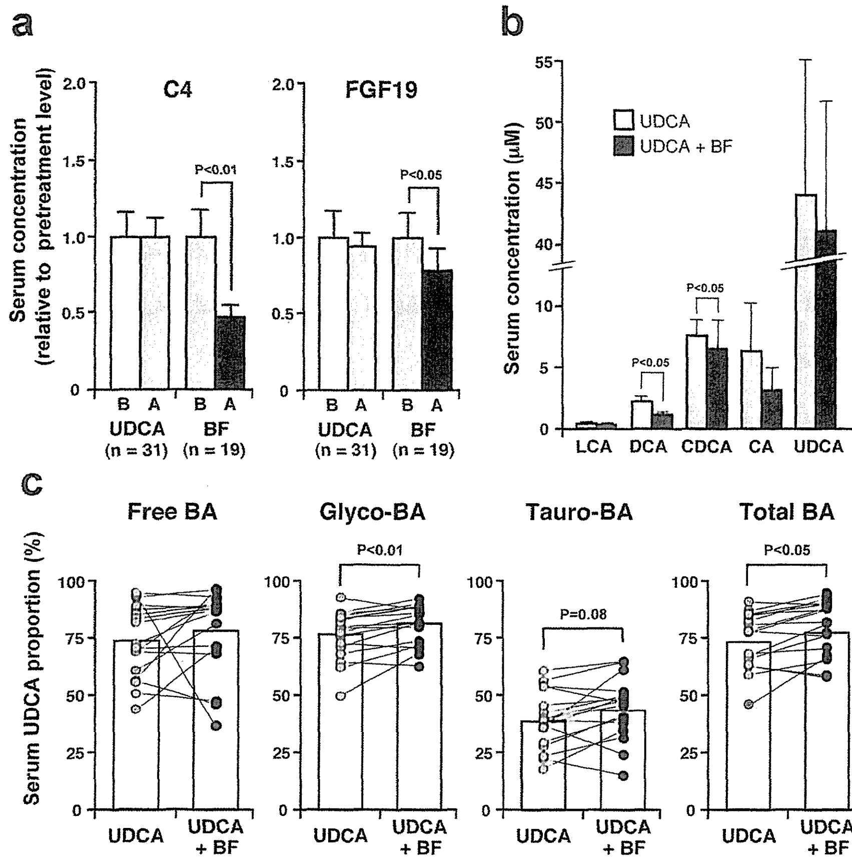


Fig. 2. Effects of UDCA and additional bezafibrate treatment on bile acid metabolism. (a) C4, 7α-hydroxy-4-cholesten-3-one; FGF19, fibroblast growth factor 19; B, before treatment; A, after treatment; BF, bezafibrate. Mean concentrations before treatment (ng/mg cholesterol for C4 and pg/ml for FGF19) were set to 1.0, and the absolute concentrations before treatment are shown in Table 2. Data are expressed as the mean±SEM. (b) Serum concentrations of bile acids in UDCA treated patients before and after addition of bezafibrate (n=17). (c) Serum proportions of UDCA in UDCA treated patients before and after addition of bezafibrate (n=17). The mean value for each group is indicated by the columns. Free BA, unconjugated bile acids; Glyco-BA, glycine-conjugated bile acids; Tauro-BA, taurine-conjugated bile acids.
176x173mm (300 x 300 DPI)

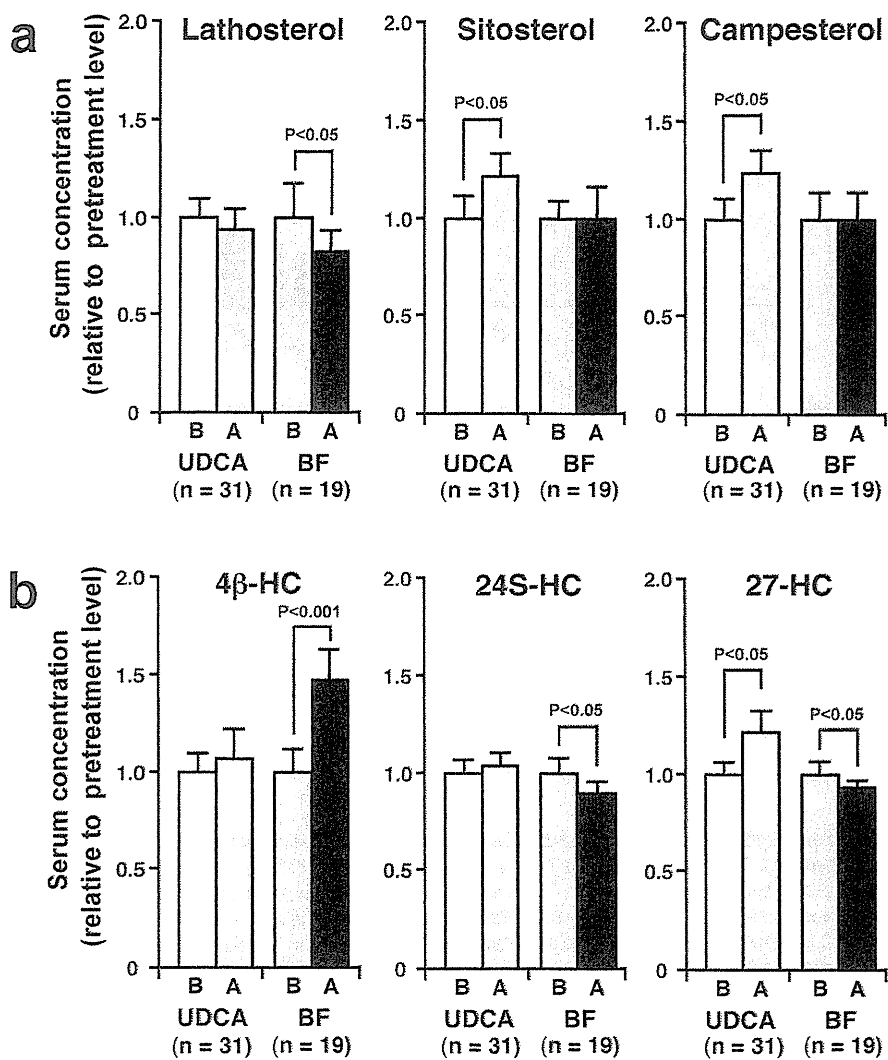


Fig. 3. Effect of UDCA and additional bezafibrate treatment on cholesterol (a) and oxysterol (b) metabolism. B, before treatment; A, after treatment; BF, bezafibrate; 4β-HC, 4β-hydroxycholesterol; 24S-HC, 24S-hydroxycholesterol; 27-HC, 27-hydroxycholesterol. Mean concentrations before treatment (μg/mg cholesterol or ng/mg cholesterol) were set to 1.0, and the absolute concentrations before treatment are shown in Table 2. Data are expressed as the mean±SEM.
131x159mm (300 x 300 DPI)

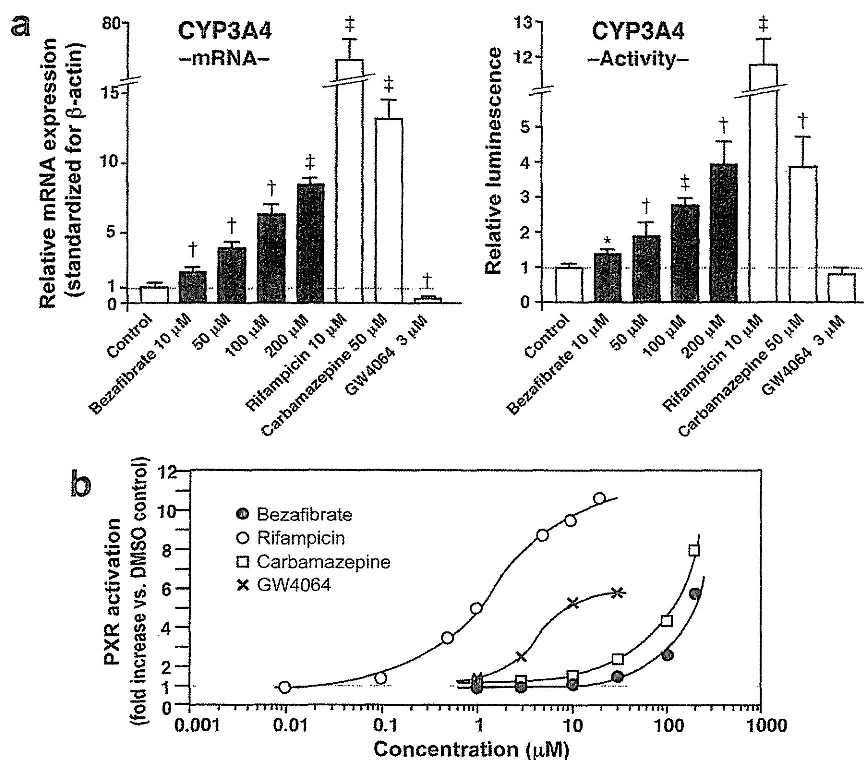


Fig. 4. Effects of bezafibrate, rifampicin, carbamazepine and GW4064 on the activation of CYP3A4 and human PXR. (a) HepaRG cells were treated with each compound for 48 hrs in triplicate. mRNA expression levels were standardized to those of β-actin. The mean expression and activity levels in control cells were set to 1.0. Data are expressed as the mean±SD. Effects of bezafibrate are shown as the solid bars. *, †, ‡ $P<0.05$, 0.005, 0.001, respectively, indicate significant difference from controls. (b) DPX2 cells were treated with each compound for 24 hrs in triplicate. Activation of human PXR was determined by a cell-based luciferase reporter gene assay. The average relative luminescent units (RLU) obtained with the DMSO solvent control was set to 1.0.
192x170mm (300 x 300 DPI)

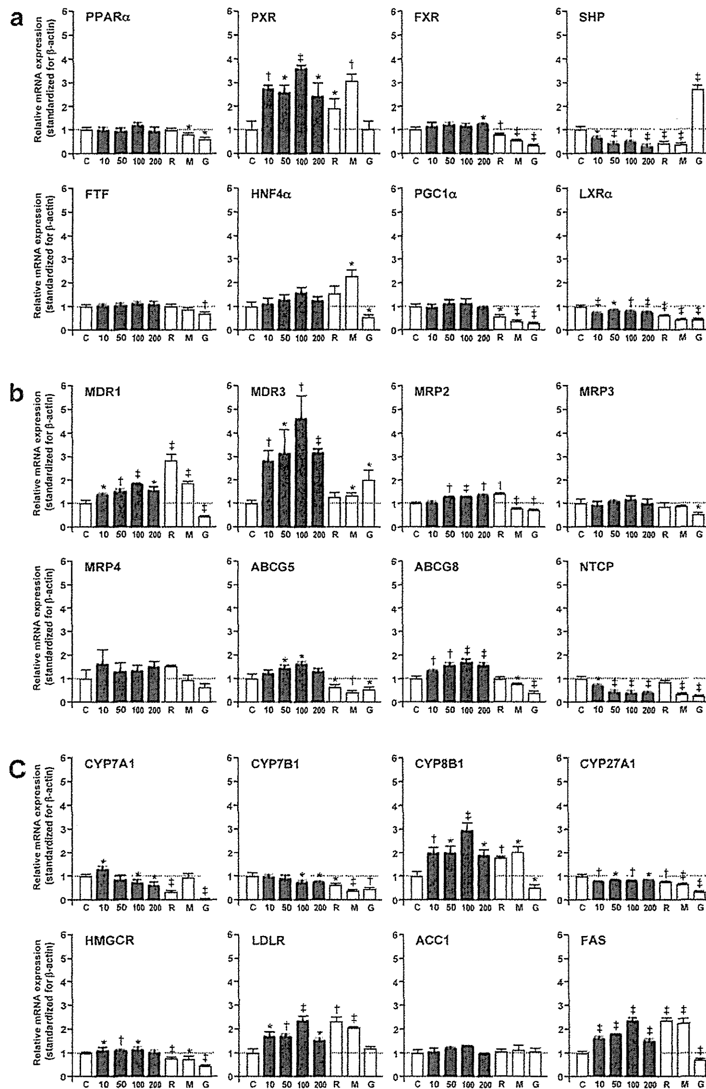


Fig. 5. Effects of bezafibrate, rifampicin, carbamazepine and GW4064 on mRNA expression levels of nuclear receptors and a related coactivator (a), transporters (b) and enzymes and LDL receptor (c) in HepaRG cells. The cells were treated with each compound for 48 hrs, in triplicate. mRNA expression levels were standardized to those of β-actin. The mean expression and activity levels in control cells were set to 1.0. Data are expressed as the mean±SD. The effects of bezafibrate are shown as the solid bars. C, control; 10, bezafibrate 10 μM; 50, bezafibrate 50 μM; 100, bezafibrate 100 μM; 200, bezafibrate 200 μM; R, rifampicin 10 μM; M, carbamazepine 50 μM; G, GW4064 3 μM. *, †, ‡ $P<0.05$, 0.005, 0.001, respectively, indicate significant difference from control.
176x277mm (300 x 300 DPI)

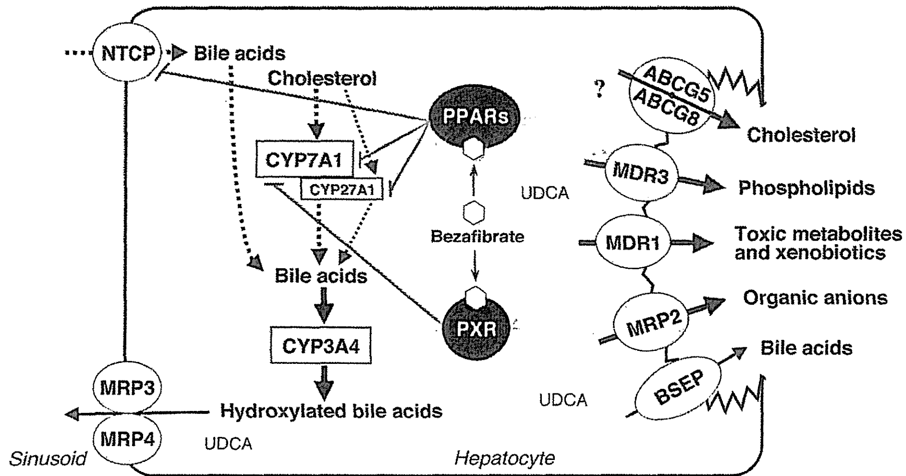


Fig. 6. Regulation of hepatic transporter activities and bile acid metabolism by PPARs, PXR and UDCA. Bezafibrate is a dual agonist of both PPARs and PXR. The activation of PPARs inhibits CYP7A1, CYP27A1 and NTCP, and upregulates MDR3 and presumably ABCG5/G8. The activation of PXR inhibits CYP7A1 and stimulates CYP3A4, MDR1 and MRP2. Genes that are downregulated by PPARs or PXR are indicated by the red lines, while those that are upregulated by PPARs, PXR or UDCA are indicated by the green arrows.
265x149mm (300 x 300 DPI)

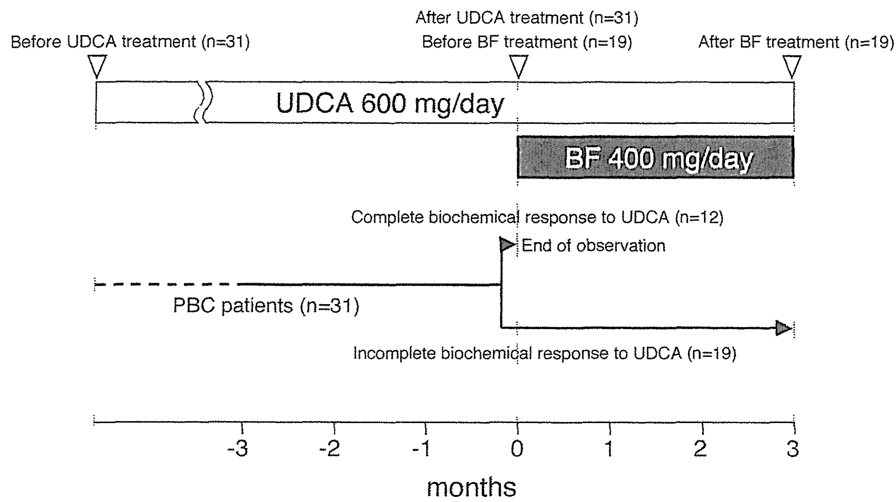


**Supporting Figure.** Treatment and blood sample collection in enrolled patients with PBC. All patients (n=31) were treated with UDCA (600 mg/day) alone for at least 3 months (maximum 6 months) until serum ALP and GGT became stable. Then, bezafibrate (BF, 400 mg/day) was administered with UDCA (600 mg/day) to patients (n=19) who exhibited an incomplete biochemical response to UDCA monotherapy and treated for 3 months.

▽, Blood sample collection for biomarker analyses.

191x169mm (300 x 300 DPI)

**Supporting Table. Primer Sequences Used in mRNA Quantification by Real-Time Reverse-Transcription PCR**

| mRNA | Genbank Accession No. | Forward | Reverse | Amplicon length (bp) |
|---|---|---|---|---|
| PPARα | AB307690 | 5'-CCATCGGCGAGGATAGTTC-3' | 5'-CGGGGACCACAGGATAAGT-3' | 144 |
| MDR3 | M23234 | 5'-ATAGCTCACGGATCAGGTC-3' | 5'-AGCACCCAATCCTGAGTAG-3' | 183 |
| MRP2 | U49248 | 5'-GACGACCATCCAAAACGA-3' | 5'-GTCCAGGGATTTGTAGCAG-3' | 152 |
| MRP3 | AF085692 | 5'-CTCCAGCTTCCTCATCAGTG-3' | 5'-GTGTTGTAAGATCAGCGACTGC-3' | 184 |
| MRP4 | AY081219 | 5'- TCGTCAGCATCCGAAGAATC-3' | 5'- AGCTAACAATTCGCCAGGTC-3' | 188 |
| ABCG5 | AF320293 | 5'-GTGCTTGTTGGATCTGGATTC-3' | 5'-GGCACACATTGGATTAGTTGTC-3' | 180 |
| ABCG8 | AF320294 | 5'-TGGTGTTTTGAAGGGCTGATG-3' | 5'-CGATGAGGTAGATGGCGTAGA-3' | 148 |
| CYP3A4 | AF182273 | 5'-TTGTCCTACCATAAGGGCTT-3' | 5'-GGCTGTTGACCATCATAAAAG-3' | 89 |
| ACC1 | NM_198834 | 5'-CAGAGACTACGTCCTCAAGCAA-3' | 5'-GTATGACTTCTGCTCGCTGA-3' | 119 |
| FAS | NM_004104 | 5'-CACCCAAGGCCAAGTACCAT-3' | 5'-GGATACTTTCCCGTCGCATA-3' | 119 |
| LDLR | AY114155 | 5'-GCTCACCACGGTGGAGATAG-3' | 5'-AATGGACAGAGCCCTCACG-3' | 103 |
| β-Actin | NM_001101 | 5'-ACTGGGACGACATGGAGAAA-3' | 5'-ATAGCACAGCCTGGATAGCA-3' | 189 |

Real-time quantitative PCR was performed as described under "Materials and Methods."

PPARα, peroxisome proliferator-activated receptor α; MDR, multidrug resistance protein; MRP, multidrug resistance-associated protein; ABC, ATP-binding cassette transporter; ACC1, acetyl-CoA carboxylase 1; FAS, fatty acid synthase; LDLR, LDL receptor.

Amino Acids
DOI 10.1007/s00726-012-1381-0

INVITED REVIEW

# Taurine and liver diseases: a focus on the heterogeneous protective properties of taurine

Teruo Miyazaki · Yasushi Matsuzaki

Received: 10 May 2012 / Accepted: 27 July 2012
© Springer-Verlag 2012

**Abstract** Taurine (2-aminoethylsulfonic acid) has many physiological and pharmacological functions in most tissues. It is abundantly maintained in the liver by both endogenous biosynthesis and exogenous transport, but is decreased in liver diseases. In the hepatic lobule, there are heterogeneous differences in metabolism between the pericentral (PC) and periportal regions, and the distributions of the biosynthesis capacity and specific taurine transporter expression are predominantly in the PC region. In cases of depletion of hepatic taurine level, serious liver damages were observed in the PC region. Taurine has protective effects against xenobiotics-induced liver damages in the PC region, but not xenobiotics-induced PP region damages. The xenobiotics that injure the PC region are mainly catabolized by NADPH-dependent cytochrome P450 2E1 that is also predominantly expressed in the PC region. Taurine treatment seems to be a useful agent for CYP2E1-related liver diseases with predominant damages in the PC region.

**Keywords** CYP2E1 · Hepatic lobule · Oxidative stress · PC region · Xenobiotics

## Introduction

The liver plays crucial roles in metabolism of many molecules, including glucose, lipids, amino acids, and xenobiotics, and these metabolic processes are each regulated by specific enzymes (Gebhardt 1992; Jungermann and Katz 1989). Since the directions of blood and bile flows and the oxygen gradient in hepatic lobules differ due to the subcellular structure of the liver acinus, these metabolic enzymes have heterogeneous patterns of expression and activity (Fig. 1). The hepatic lobule, defined as Kiernan's classical lobule, is histologically divided into three regions: the periportal (PP, zone 1) region around the portal vein, the pericentral (PC, zone 3) region around the central vein, and the intermediate (zone 2) region (Kiernan 1833). The metabolic characteristics of hepatocytes differ in the PP and PC regions. In the PP region, oxidative energy metabolism, amino acid catabolism, ureagenesis, gluconeogenesis, cholesterol synthesis, $\beta$-oxidation, and bile formation are predominant, whereas glycolysis, glycogenesis, liponeogenesis, ketogenesis, glutamine formation, and xenobiotic metabolism are preferentially situated in the PC region (Fig. 1; Jungermann and Katz 1989). In liver diseases, hepatocellular damage including necrosis and apoptosis, fatty degeneration, inflammation, and fibrosis have histological differences in etiology, including virus infection, metabolic disorder, immunological response, and drug metabolism. In rat hepatocytes, there is a zonal heterogeneous distribution of taurine (2-aminoethanesulfonic acid) within one hepatic lobule (Penttila 1990), and the variation of taurine levels between the PP and PC regions seems to be an important determinant of susceptibility to zonal toxic responses. The normal level of hepatic taurine content is 4–11 μmol/g wet weight, and the content can be varied by exogenous administrations of taurine (Penttila 1990) or $\beta$-alanine, which is an antagonist for a specific transporter of taurine (Kim and Kim 2002; Pacioretty et al. 2001; Parildar-Karpuzoglu et al. 2007), and in gene knockout of the specific transporter (Warskulat et al. 2006).

T. Miyazaki (✉)
Joint Research Center, Tokyo Medical University Ibaraki Medical Center, Ami, Japan
e-mail: teruom@tokyo-med.ac.jp

Y. Matsuzaki
Division of Gastroenterology and Hepatology, Department of Internal Medicine, Tokyo Medical University Ibaraki Medical Center, Ami, Japan

Published online: 24 August 2012

Many studies have demonstrated the therapeutic efficacy of taurine for liver diseases including inflammatory condition, apoptosis, and fibrosis through anti-oxidative stress action (Chen et al. 2004; Kato et al. 2004; Miyazaki et al. 2005; Refik Mas et al. 2004). Furthermore, various symptoms related to liver diseases including jaundice in acute hepatitis (Matsuyama et al. 1983) and hepatic encephalopathy (Butterworth 1996) and muscle cramp (Matsuzaki et al. 1993; Yamamoto 1994) in cirrhotic patients have been reported to be improved by taurine treatment. In this review, we will mainly discuss the relationship of heterogeneous liver diseases with the distribution and regulatory functions of taurine in the hepatic lobules.

## Taurine homeostasis in the liver

Taurine is the most abundant free amino acid-like compound found in mammalian tissues, including liver (Awapara 1956; Huxtable 1980; Jacobsen and Swimth 1968; Sturman 1993). In the liver, the most established role of taurine is its conjugation with bile acids for excretion into bile (Danielsson 1963; Sjovall 1959). However, taurine has many other physiological and pharmacological roles in the liver and other tissues, including stabilization of the cellular plasma membrane (Pasantes et al. 1985), osmoregulation (Nieminen et al. 1988), anti-oxidant effects (Nakamura et al. 1993), and detoxification (Huxtable 1992). High intracellular levels of taurine are maintained by exogenous uptake and endogenous synthesis. Taurine is an end product in sulfur amino acid catabolism through the methionine and cysteine pathways in the liver (Bella et al. 1999a, b; De La Rosa and Stipanuk 1985). In this taurine biosynthesis pathway, cysteine dioxygenase (CDO) (Hosokawa et al. 1990) and cysteine sulfinate decarboxylase (CSD) (Kaisaki et al. 1995; Reymond et al. 1996; Tappaz et al. 1999) are key limited enzymes. An excellent anti-oxidant agent glutathione (GSH; L-γ-glutamyl-L-cysteinylglycine) also utilizes cysteine in the biosynthesis pathway (Meister and Anderson 1983). Penttila (1990) investigated the heterogeneities and regulation of taurine, cysteine and GSH concentrations using [35S] cysteine in hepatocytes isolated separately from the PC and PP regions, respectively, by a digitonin/collagenase perfusion technique that can destroy the respective regions by perfusion of digitonin from the portal vein or inferior vena cava. The resulting

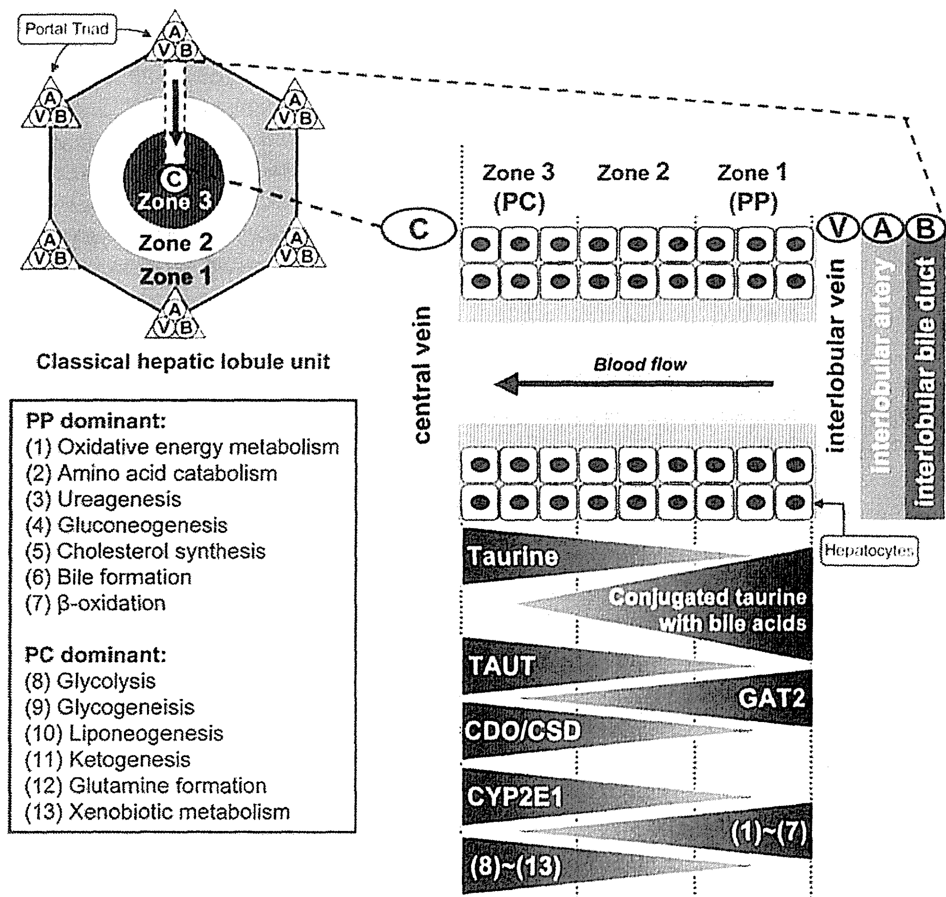


**Fig. 1** Heterogeneous distributions of hepatic metabolisms, taurine level, and its maintenance capacities in the hepatic lobule. The hepatic lobule is divided into three regions as zone 1–3 by Kiernan's classical lobule classification. Taurine level, the capacities of taurine biosynthesis, the protein expressions of TAUT, and the cytochrome P450 isoform 2E1 expression in the hepatic lobule are predominant in zone 3, while uptake of taurine through GAT2, GAT2 protein expression, and taurine conjugation with bile acids are predominant in zone 1. *C* central vein, *V* interlobular vein, *A* interlobular artery, *B* interlobular bile duct, *Zone 1* periportal region, *Zone 2* intermediate region, *Zone 3* pericentral region, *TAUT* taurine transporter, *GAT2* GABA transporter 2, *CDO* cysteine dioxygenase, *CSD* cysteine sulfinate decarboxylase, *CYP2E1* cytochrome P450 2E1

taurine content in the PC hepatocytes was higher (1.9 ± 1.4 μmol/g of cells) than in the PP hepatocytes (1.1 ± 0.5 μmol/g). Along with faster uptake of [35S] cysteine into the PC hepatocytes, the rate of taurine production from [35S] cysteine in the PC hepatocytes was sevenfold higher than in the PP hepatocytes. Furthermore, Parsons et al. (1998) showed that the expression of CDO protein was predominantly localized in the PC region of rat liver by immunohistological stain. In addition to endogenous synthesis, the taurine content in the liver and other tissues is also maintained by the exogenous diet through uptake via a specific transporter (TAUT; SLC6A6) (Han et al. 2006; Liu et al. 1992; Smith et al. 1992; Uchida et al. 1992). The zonal distribution of TAUT in hepatic lobules is unclear. Our unpublished immunohistochemical staining data show that TAUT in rat hepatic tissue is also predominantly and markedly expressed in the PC rather than the PP region (Fig. 2; see figure legend for the detailed method). These observations indicate that the basal content, product capacity, and transport ability of taurine within the hepatic lobule are higher in the PC region than in the PP region. On the other hand, the study by Penttila (1990) showed that cellular GSH synthesis from endogenous precursor (cysteine) was faster in the PP hepatocytes than in the PC hepatocytes. The distribution of GSH in the hepatic lobule implies that the capacity of detoxication in the PP region is higher than in the PC region, although activation of numerous xenobiotics to reactive metabolites predominates in the PC region via cytochrome P450 isoform 2E1 (CYP2E1) that were highly expressed in the PC region (Lieber 1997; Fig. 2). Therefore, it has been suggested that hepatocytes in the PC region might be limited in detoxication process due to the lower capacity to replenish GSH and, consequently, the PC region easily sustains damages from the electrophilic metabolites (ROS) of CYP2E1.

## Taurine homeostasis and liver diseases

Morphological abnormalities and incomplete tissue development have been observed in the liver and in other tissues in taurine-deficient animal models (Han et al. 2000; Ito et al. 2008; Neuringer et al. 1987; Sturman 1993; Sturman and Messing 1991; Warskulat et al. 2006). Since the capacity for taurine biosynthesis is generally limited in humans and rodents, a deficiency of taurine in the liver seems to be caused by decreased uptake of exogenous taurine, rather than dysfunctions of endogenous biosynthesis. Häussinger's group has created homozygous (*taut*$^{-/-}$) and heterozygous (*taut*$^{+/-}$) models of TAUT knockout mice (Heller-Stilb et al. 2002; Lang et al. 2003; Warskulat et al. 2004, 2006). In the *taut*$^{-/-}$ mouse, the knockout of TAUT induced taurine depletion in a variety of tissues, including decreases of ~74 % in plasma, kidney, and eye, and of >95 % in skeletal muscle and heart at 2–19 months of age. These changes were associated with a lower body mass, reduced fertility, and loss of vision with severe apoptotic retinal degeneration. In the liver, the taurine concentration in 2-month-old *taut*$^{-/-}$ mice (1.6 ± 0.4 μmol/g) were decreased by >40 and >90 % compared to that in *taut*$^{+/-}$ (12.1 ± 2.0 μmol/g) and *taut*$^{+/+}$ (17.7 ± 2.5 μmol/g), respectively, accompanied with a reduction of the liver wet weight (Warskulat et al. 2006). The *taut*$^{-/-}$ mice also had hepatitis with hepatocyte destruction, apoptosis, fibrosis, mitochondrial abnormalities, and an increased frequency of neoplastic lesions predominantly in the PC regions of hepatic lobules beyond 1 year of age. Since TAUT was predominantly expressed in the PC region (Fig. 2), the homeostasis of taurine seems to be an important factor for heterogeneous hepato-protection in this region.

Interestingly, the reduction of taurine content in the liver of TAUT KO mice was more mild compared to that in nonparenchymal cells such as Kupffer cells and sinusoidal endothelial cells and in other tissues (Warskulat et al. 2006). One of the reasons for this might be the taurine synthesis ability in the liver, but Ikeda et al. (2012) recently showed the importance of γ-aminobutyric acid (GABA) transporter 2 (GAT2) in the uptake of taurine into the liver. Similar to TAUT, GAT2 which is a rat ortholog of human GAT3 belongs to a family of $Na^+/Cl^-$-dependent neurotransmitter transporters and has lower affinity ($K_m = 540$ μM) (Liu et al. 1993) compared to TAUT ($K_m = 43$ μM) (Smith et al. 1992). Ikeda et al. (2012) confirmed that taurine could be transported into hepatocytes through GAT2, because the uptakes of [$^3$H] taurine injected into the portal vein in anesthetized rat and of [$^3$H] taurine exposed to freshly isolated hepatocytes were significantly inhibited by the antagonists for GAT2. Furthermore, immunohistochemical analysis showed that GAT2 protein was localized on the sinusoidal membrane of hepatocytes, predominantly in the PP region (Ikeda et al. 2012). These observations imply that the enterohepatic circulation of taurine and bile acid conjugated with taurine are regulated by GAT2 in the PP region. Therefore, the authors proposed one explanation for the discrepancy that taurine synthesis was higher in the PC region, but taurine conjugation with bile acids was higher in the PP region (Ikeda et al. 2012). They suggested that oral taurine treatment could be a useful therapy for cholestatic disease, because the conjugation composition of bile acids would be changed from more cytotoxic glycine-conjugated bile acids to taurine-conjugated bile acids. Compared to the evidence reported by Penttila (1990), it has been considered that free taurine is abundant in the PC region, while taurine

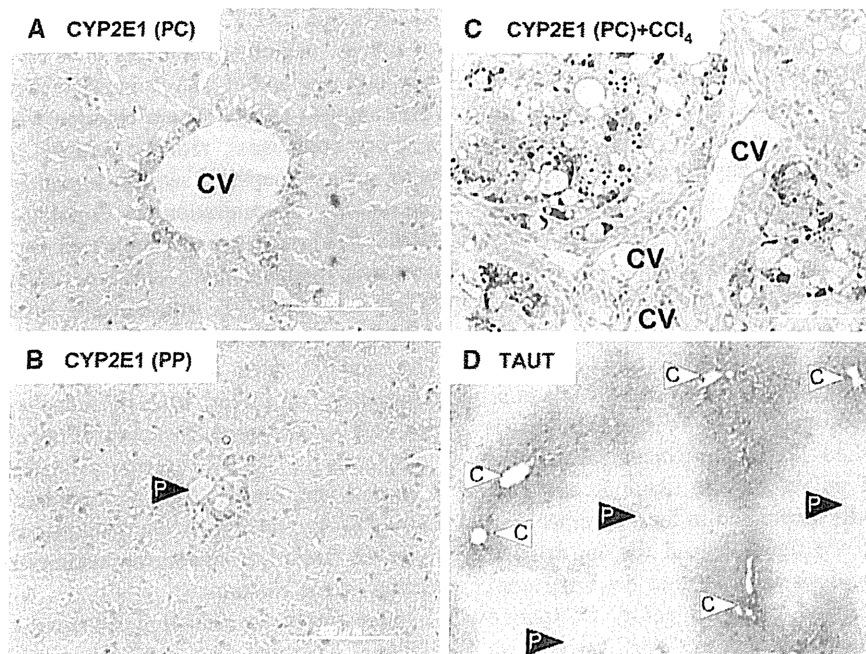


**Fig. 2** Heterogeneous protein expressions of CYP2E1 and TAUT in the hepatic lobule of normal and $CCl_4$-administered hepatic tissues in rats on immunohistochemical stain. Hepatic tissues collected from normal or liver-damaged rats that received $CCl_4$ administration were immunohistochemically stained with a rabbit anti-TAUT (Alpha Diagnostic International, Inc., San Antonio, TX, USA) or anti-CYP2E1 (Millipore, Bedford, MA, USA) primary antibodies and biotin-conjugated universal secondary antibody (Ventana, Tucson, AZ, USA). **a** CYP2E1 expression in hepatocytes around the central vein of normal tissue (×10). **b** very weak or no expression of CYP2E1 in the PP region of normal tissue (×10). **c** Activated CYP2E1 expression in the PC region with cell damages, fat droplets, and fibrosis by chronic administration of 50 % $CCl_4$–olive oil solution for 10 weeks (×20). **d** TAUT protein expression dominantly in the PC region of normal tissue (×2). *CV* central vein, *C in the white arrow* central region, *P in the block arrow* portal region

transported by GAT2 in the PP region is preferentially utilized to conjugation with bile acids (Fig. 1).

Administration of $\beta$-alanine, an inhibitor of taurine uptake on TAUT, is also used to prepare animal models of taurine depletion in liver and other tissues (Kim and Kim 2002; Parildar-Karpuzoglu et al. 2007). Depending on the protocol, dose, and duration of $\beta$-alanine administration, the taurine level is decreased by approximately 20–85 %, with the greatest change in the liver among all tissues (Pacioretty et al. 2001). Taurine depletion in the liver has been suggested to be due to reduced taurine uptake into hepatocytes, and Shaffer and Kocsis (1981) also showed that $\beta$-alanine administration enhanced excretion of taurine into urine because of competition of $\beta$-alanine with taurine for re-uptake in renal tubules. In contrast to TAUT knockout mice, histopathologic changes in the liver were not found in taurine depletion models induced by $\beta$-alanine administration. However, co-administration of $\beta$-alanine with hepatotoxins such as ethanol (EtOH) or carbon tetrachloride ($CCl_4$) causes aggravation of hepatic dysfunction, impairment, and fibrosis, together with significant hepatic taurine depletion (Erman et al. 2004; Kerai et al. 2001; Waterfield et al. 1993; Wu et al. 2009). This suggests that $\beta$-alanine does not have a protective effect against hepatotoxins. However, there are conflicting findings on the protective effects of $\beta$-alanine against liver damage caused by $CCl_4$ or lipopolysaccharide through enhanced biosynthesis of taurine and GSH in the liver (Kim and Kim 2002; Lee and Kim 2007), and further studies are needed to clarify this issue.

## Overview: heterogeneous protective actions of taurine against hepatotoxins

In liver diseases, the extent of reduction of the hepatic taurine concentration depends on the degree of symptoms, including loss of hepatocytes, inflammation, fibrosis, and fatty degeneration. Taurine concentration in plasma and urine has been proposed to be a biomarker of liver damage, because elevation of taurine concentration in plasma and urine was found following hepatotoxin overdose due to leakage from damaged hepatic cells (Ghandforoush-Sattari and Mashayekhi 2008; Waterfield et al. 1991). In many in vivo studies, taurine administration has been shown to protect hepatic tissue and hepatocytes against various substrates, inducing hepatotoxicities, oxidative stress, and hepatocarcinogenesis (Balkan et al. 2001, 2002; Bleich and

Degner 2000; Dinçer et al. 2002; Dogru-Abbasoglu et al. 2001; Erman et al. 2004; Kerai et al. 1999; Miyazaki et al. 2005; Nakashima et al. 1982; Pushpakiran et al. 2004; Waters et al. 2001; You and Chang 1998). In these studies, there are common features of damage to the hepatic lobule occurring predominantly in the PC region and major metabolism of hepatotoxins by CYP2E1 (Konishi and Ishii 2007; Lieber 1997). CYP2E1 has the highest expression among all CYP isoforms in human liver and also the highest in the liver among other tissues (Bieche et al. 2007). It is the principal P450 for the metabolism of xenobiotics including EtOH, acetaldehyde, acetaminophen (APAP; paracetamol), acrylamide, aniline, benzene, butanol, $CCl_4$, dimethylether, dimethyl sulfoxide, ethyl carbamate, ethylene chloride, halothane, glycerol, ethylene glycol, *N*-nitrosodimethylamine, 4-nitrophenol, pyrazole, pyridine, thioacetamide (TAA), and vinyl chloride (Delaney and Timbrell 1995; Guengerich et al. 1991; Kang et al. 2008; Konishi and Ishii 2007; Lee et al. 1996; Slater et al. 1985; Sohn et al. 1991; Wilson et al. 1996). Most metabolites produced in the metabolism of these molecules by CYP2E1 are hepatotoxins that cause oxidative stress and membrane lipid peroxidation (Gonzalez 2005; Fig. 3). Therefore, the hepato-protective action of taurine might be strongly related to the reduction of CYP2E1 metabolic activity or consequent oxidative stress in the hepatotoxin-induced liver damage in the PC region. On the other hand, taurine has very little or no protective effect against toxic agents such as allyl alcohol and α-naphthylisothiocyanate, which induce liver injury predominantly in the PP region (Jung et al. 2000; Mehendale et al. 1994). Allyl alcohol is metabolized in an oxygen-dependent manner to a highly hepatotoxic aldehyde (acrolein) by the action of alcohol dehydrogenase, which is located predominantly in the PP region (Reid 1972; Serafini-Cessi 1972). Since oxidative stress involving lipid peroxidation in hepatocytes with mitochondrial dysfunction has been postulated as a major mechanism in allyl alcohol hepatotoxicity, similarly to the model of $CCl_4$-induced liver damage, heterogeneous protective action of taurine as anti-oxidative stress may depend on the distribution and homeostasis of taurine within the hepatic lobule.

## Protective effect of taurine on $CCl_4$-induced liver damage

Models of acute and chronic liver disease induced by $CCl_4$ administration are well established in rodents (Ariosto et al. 1989; Holecek et al. 1999; Perez Tamayo 1983). $CCl_4$ is converted to a trichloromethyl radical ($CCl_3^{\cdot}$), mainly by CYP2E1 in the hepatocyte endoplasmic reticulum membrane, and the free radical subsequently causes hepatic injury in the PC region (Slater et al. 1985; Fig. 3). The effectiveness of taurine against $CCl_4$-induced liver disease in rats has been reported widely (Erman et al. 2004; Nakashima et al. 1982; Wu et al. 1999). In an acute liver disease model in rat induced by a single administration of $CCl_4$, Dinçer et al. (2002) showed that taurine treatment prevented hepatocellular necrosis, lipid peroxidation, and mitochondrial abnormalities observed by electron microscopy. In a chronic hepatic disease model, we showed that oral taurine administration significantly improved the serum levels of aminotransferases and bilirubin; the histological appearance in the PC region including cell necrosis, fatty degeneration, and inflammation; and oxidative stress markers in serum and hepatic tissue including lipid hydroperoxides and 8-hydroxy-2′-deoxyguanosine (Miyazaki et al. 2005). Taurine also significantly decreased hepatic fibrosis induced by $CCl_4$ administration and fibrogenesis of isolated hepatic stellate cells, which are converted to myofibroblasts by oxidative stress in cirrhotic liver, through inhibition of transforming growth factor-β expression. In $CCl_4$-administered rats, the taurine concentration in the liver, plasma, and other tissues was significantly decreased (Miyazaki et al. 2004), but the decreased hepatic taurine concentration can be improved by oral taurine administration (Miyazaki et al. 2005; Nakashima et al. 1982). Indeed, Erman et al. (2004) reported that the significant decrease of hepatic taurine concentration in the $CCl_4$-administered rat together with ethanol was significantly recovered by 2 % taurine-containing drinking water, while the significant decrease was not improved by 3 % β-alanine drinking water. The decreased taurine concentration in the liver might be associated with a significant decrease in TAUT protein in the damaged liver tissue; however, it is unclear whether oral taurine administration could upregulate the transport ability of taurine or not.

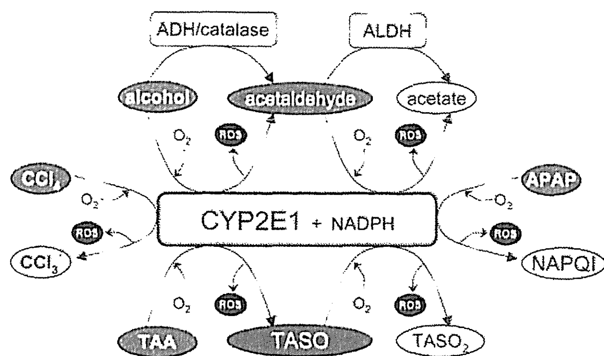


**Fig. 3** Catabolic pathways of xenobiotics by cytochrome P450 2E1. ROS are generated in the CYP2E1-mediated reactions. *ADH* alcohol dehydrogenase, *ALDH* acetaldehyde dehydrogenase, *APAP* acetaminophen, *$CCl_4$* carbon tetrachloride, *$CCl_3^{\cdot}$* trichloromethyl radical, *NAPQI N*-acetyl-*p*-benzoquinone imine, *TAA* thioacetamide, *TASO* thioacetamide sulfoxide, *$TASO_2$* thioacetamide-*S,S*-dioxide